01

Calculation of axisymmetric current systems using the model of an axially magnetized cylinder

© A.K. Andreev

Moscow Aviation Institute National Research University,
125993 Moscow, Russia
e-mail: alexande_andreev@yahoo.com

Received May 2, 2023
Revised December 14, 2023
Accepted December 24, 2023

A method for calculating the inductive and power parameters of complex coaxial axisymmetric current systems based on a cylinder model is proposed. The method is based on the equivalence of the energies of coils and equal-sized cylinders with equal densities of their surface currents. The inductances, mutual inductances and ponderomotive forces in the coil system are calculated from the mutual energy and 3D fields of the cylinders. It is shown that the volume-average demagnetizing factor of a cylinder is equivalent to the Nagaoka coefficient for the inductance of coils of finite length. From the analysis of the correlation between the energy densities of the cylinder and the demagnetization energy, the criterion of a „short coil" is determined. The correspondence of the results obtained by the cylinder model to the calculations by current models is established. A method for calculating interlayer mechanical stresses, mutual radial and axial forces and stresses in a system of coaxial coils (cylinders) is presented. An example of using a cylinder model for calculating the inductance of a rectangular coil is given.

Keywords: demagnetizing factor, Nagaoka coefficient, coil, inductance, energy, mechanical stresses.

DOI: 10.21883/0000000000

Intoduction

Inductive and power (ponderomotive) characteristics are the most important parameters of magnetic systems The term „solenoid" is usually used to describe a type of coil whose length is much greater than its diameter. Force interactions in axisymmetric magnetic systems are usually calculated for current systems: coils and solenoids. Calculations of ponderomotive forces are necessary when creating high-intensity pulsed magnetic fields [1–6]. The specified literature is devoted to the technical implementation of the assigned tasks with an emphasis on the strength characteristics of products The calculations use approximate formulas for magnetic fields obtained for current systems. The complexity of calculating coil fields leads to the need to simplify problems and present results using series, approximating formulas, or graphic-analytical methods [4,5]. The difference in parameter values calculated using different methods can be several percent, which is considered quite acceptable. Extended information on methods for calculating coils can be found on the Internet at the sites [7], where links to primary sources are also provided.

The single-layer coil plays a special role in the design of magnetic systems. On its basis, complex multicomponent systems are calculated. Methods for calculating the inductance of single-layer coils through elliptic integrals were first developed by J.C. Maxwell for windings made of round wire [8] and L. Lorentz for coils of ribbon conductors [9]. These results have the same meaning for electrical and radio engineers as Maxwell's electromagnetic field equations do for physicists. Nagaoka redefined the Maxwell-Lorentz formulas by introducing the concept of the geometric factor of the coil shape [10]. ow the elliptic integrals contained instead of parameters: „coil length h — diameter $2a$", their ratio $h/2a$.

With the introduction of the Nagaoka coefficient, the inductance of a single-layer coil is written as follows:

$$L = \left(\mu_0 \frac{w^2}{h} \frac{\pi(2a)^2}{4}\right) k_L, \ (0 \le k_L \le 1), \qquad (1)$$

where μ_0 — permeability of vacuum,w — quantity of coil turns, k_L — Nagaoka coefficient. The expression in parentheses determines the inductance L_h of the solenoid section with length h.

The energy accumulated in the coil is

$$E_{coil} = I^2 L/2, \qquad (2)$$

where I is current in the coil turn.

Nagaoka coefficient introduces a correction for the finite length of the coil and in Lorentz form has the form

$$k_L = \frac{8a}{3\pi h}\left(\frac{2k-1}{k^3} E_c(k) + \frac{1-k^2}{k^3} K_a(k) - 1\right), \qquad (3)$$

where$K_a(k)$ and $E_c(k)$ — complete elliptic integrals of the 1st and 2nd kind:

$$K_c(k) = \int_0^{\pi/2} \frac{1}{\sqrt{1-k^2\sin^2\theta}}\, d\theta,$$

$$E_c(k) = \int_0^{\pi/2} \sqrt{1-k^2\sin^2\theta}\, d\theta,$$

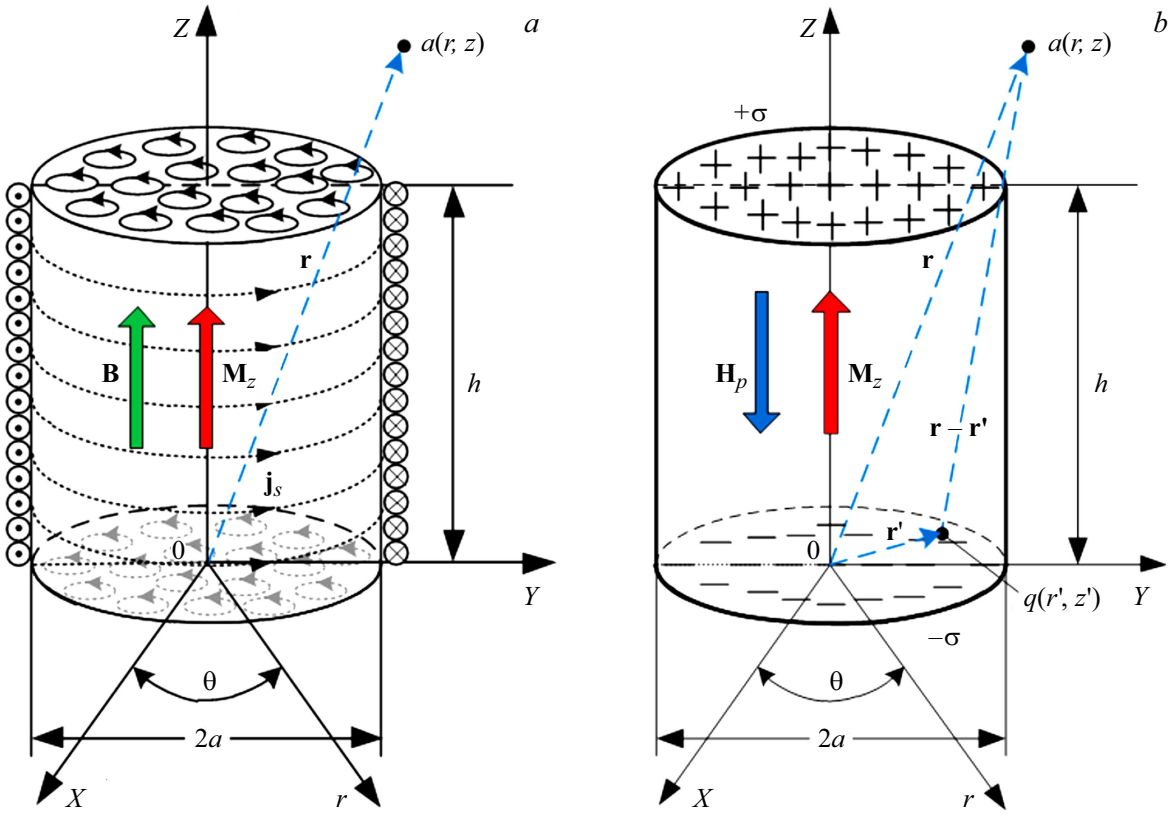

Figure 1. *a* — scheme for determining induction **B**; *b* — scheme for calculating the field of a cylinder $\mathbf{H}_p$. The hatched coordinates $q(r', z')$ are associated with the field source point. The symbol $a(r, z)$ indicates the observation point.

with $k = 2a(4a^2 + h^2)^{-1/2}$ module.

The inhomogeneity of the induction of short coils significantly complicates the calculations. Numerous examples of calculations of practical systems are discussed in the reference book [11]. Direct numerical methods for calculating the inductive parameters of coils without converting the original integral expressions into algebraic ones are given in [12].

Fields for internal regions of axisymmetric magnetic systems were obtained in [13,14]. Formulas and programs for calculating demagnetizing and 3*D* fields of cylinders during azimuthal magnetization (or induction of equivalent coils) throughout space, expressed through elliptic integrals, were published in [15]. Analytical expressions for the3*D* fields of a cylinder for arbitrary magnetization orientation were published in [16,17].

Direct calculation of inductances and mutual inductances of rectangular coils as current systems is complex and leads to extremely cumbersome formulas, which makes their use for practical calculations difficult [18–21].

This work discusses methods for calculating the inductance of coils, mutual inductance and ponderomotive forces of a densely wound coil system using an alternative method through the 3*D* fields of an axially magnetized cylinder. The winding density criterion is given in [22]. The method is based on the equality of the internal energies of the coils and their equivalent axially magnetized cylinders In fact, to calculate the basic parameters of coils, there is no need to involve labor-intensive methods of theoretical electrical engineering and magnetostatics for current systems, if only the equality of the surface current densities of coils and cylinders is established. When using a cylinder model, the calculation of a number of basic parameters of axisymmetric magnetic and current systems is significantly simplified.

1. Computational model

1.1. Basic relationships of model quantities

The coil, the cylinder axially magnetized in the z direction, and the coordinate systems associated with them are shown in Fig. 1.

The magnetization of the cylinder $\mathbf{M}_z$, the surface current density of the cylinder $\mathbf{j}_s$ and the surface „magnetic charges“ are related by the relations [23] $\mathbf{j}_s = \mathrm{Rot}\,\mathbf{M}_z$, $\sigma = -\mathrm{Div}\,\mathbf{M}_z$. With uniform magnetization $\mathbf{M}_z = \mathrm{const}$) $\mathbf{J}_s = [\mathbf{M}_z\mathbf{n}]$ (Fig. 1, *a*), $\sigma = \mathbf{M}_z\mathbf{n}$ (Fig. 1, *b*); $\mathbf{n}$ — outer normal to the surface of the cylinder. In scalar notation we have

$$M_z = j_s, \quad \sigma = M_z. \tag{4}$$

For given coil parameters — length h, diameter $2a$, number of turns w and current per turn I, the current

density of the winding is $j = wI/h$. Under the assumption $j_s = j$, the equivalent magnetization of an equidimensional cylinder is equal $M_z = j$ (Fig. 1, *a*), which ensures equality of inductances of the coil $\mathbf{B}_{coil}$ and cylinder $\mathbf{B}_{cyl}$ throughout the entire space

The fields in the volumes of the coil and cylinder are radically different. According to the dipole („charge") model of magnetization, surface „magnetic charges" $\pm\sigma$ (arise at the ends of a uniformly magnetized cylinder (Fig. 1, *b*). „Charges" create a demagnetizing field $\mathbf{H}_p$n the volume of the cylinder, directed oppositely $\mathbf{M}_z$, and a stray field outside it, also denoted by the symbol $\mathbf{H}_p$.

The demagnetizing field $\mathbf{H}_p$ plays a vital role in the calculations of magnetic systems. $\mathbf{H}_p$ is determined through the demagnetization factor of the sample $N_p(\mathbf{r})$.

1.2. Demagnetizing factor and 3*D*of the field of axially magnetized cylinder

Fields $\mathbf{H}_p(\mathbf{r})$ inside and outside a ferromagnet of arbitrary shape with a known magnetization distribution $\mathbf{M}(\mathbf{r}')$ are calculated through the gradient of the magnetostatic potential $\varphi(\mathbf{r})$ at the observation point$a(r, z)$ (Fig. 1, *b*):

$$\mathbf{H}_p(\mathbf{r}) = -\nabla\varphi(\mathbf{r}) = -\nabla \int\limits_{V'} \mathbf{M}(\mathbf{r}')\nabla' \frac{1}{|\mathbf{r}-\mathbf{r}'|}\, d^3\mathbf{r}',$$

where $\mathbf{r}'$ is radius vector of the source point $q(r', z')$, $\mathbf{r}$ are radius vectors of the observation point $a(r, z)$. The primed and unprimed operators mean differentiation with respect to $q(r', z')$ and $a(r, z)$ respectively; $d^3\mathbf{r}'$ means a volume element. When calculating the potential $\varphi(\mathbf{r})$, the equalities $\nabla'(1/|\mathbf{r}-\mathbf{r}'|) = (\mathbf{r}-\mathbf{r}'/|\mathbf{r}-\mathbf{r}'|^3) = -\nabla(1/|\mathbf{r}-\mathbf{r}'|)$are used.

With a uniformly magnetized ferromagnet, $\mathbf{M}(\mathbf{r}') = \mathbf{M} = \text{const}$, $\mathbf{H}_p(\mathbf{r})$ is written in the form [24]:

$$\mathbf{H}_p(\mathbf{r}) = V(\mathbf{M}\nabla) \int\limits_V \frac{d\mathbf{r}'}{|\mathbf{r}-\mathbf{r}'|} = -\hat{N}(\mathbf{r})\mathbf{M}, \qquad (5)$$

where$0 \le \hat{N}(\mathbf{r}) \le 1$ is tensor of demagnetizing coefficients (factors) with components

$$N_{ij}(\mathbf{r}) = -\frac{\partial^2}{\partial x_i \partial x_j} \int\limits_V \frac{d\mathbf{r}'}{|\mathbf{r}-\mathbf{r}'|}.$$

Thex_i, x_J variables are determined by the coordinate system used; $\hat{N}(\mathbf{r})$ — dimensionless quantity determined by the shape of the sample establishes proportionality between $\mathbf{H}_p(\mathbf{r})$ and $\mathbf{M}$. The potential of $\varphi(\mathbf{r})$ in the inner and outer areas of the cylinder is determined differently. Outside the cylinder, the demagnetization factor $\hat{N}(\mathbf{r})$ is zero by definition, but is a coefficient that determines the stray field. The demagnetizing field $\mathbf{H}_p(\mathbf{r}')$ is inhomogeneous throughout the sample volume and depends on its shape and magnetization, i.e. is a function of the coordinates $\mathbf{r}'$.

With uniform magnetization of the cylinder along the axis Z $M_z = \text{const}$:

$$H_p(\mathbf{r}) = -M_z \left[\nabla \int\limits_{V'} \boldsymbol{\alpha}_z \nabla' \frac{1}{|\mathbf{r}-\mathbf{r}'|}\, dV'\right] = -M_z\hat{N}(\mathbf{r}), \quad (6)$$

where$\boldsymbol{\alpha}_z$ —- unit vector of the magnetization direction. Hence the components of the demagnetizing field follow

$$H_{pi} = -N_{iz}M_z, \quad i = r, z.$$

Subsequent calculations were performed in a cylindrical coordinate system. For convenience of calculations, an auxiliary „magnetostatic potential" of two disks is introduced, which has the dimension of length [14]:

$$\psi_1(\mathbf{r}) = \int\limits_{V'} \nabla' \frac{1}{|\mathbf{r}-\mathbf{r}'|}\, dV' = \int\limits_0^a r'dr' \int\limits_0^{2\pi} d\theta'$$

$$\times \left[\begin{array}{c} \dfrac{1}{\sqrt{r^2 + r'^2 + (h-z)^2 - 2rr'\cos(\theta-\theta')}} \\ -\dfrac{1}{\sqrt{r^2 + r'^2 + z^2 - 2rr'\cos(\theta-\theta')}} \end{array}\right],$$

$$0 \le z \le h \wedge |r| \le a.$$

Applying the Lipschitz integral and the addition theorem for Bessel functions to (9), we obtain the total potential of the oppositely charged end surfaces of the cylinder [25,26]:

$$\psi_1(r, z) = 2\pi a \int\limits_0^\infty J_0(tr)J_1(ta)[e^{-tz} + e^{-(h-z)}]\frac{dt}{t},$$

$$(0 \le z \le h) \wedge |r| \le a,$$

where $J_0(tr)$ and $J_1(ta)$ — zeroth and first order Bessel functions of the real argument. Finally, we obtain formulas for the demagnetizing factors of the internal region of the cylinder:

$$N_{zz}(r, z) = -\frac{\partial}{\partial z}\psi_1(r, z) = \frac{1}{2}a \int\limits_0^\infty J_0(tr)J_1(ta)$$

$$\times [e^{-tz} + e^{-(h-z)}]dt, \quad 0 \le z \le h \wedge |r| \le a, \qquad (7)$$

$$N_{rz}(r, z) = -\frac{\partial}{\partial r}\psi_1(r, z) = -\frac{1}{2}a \int\limits_0^\infty J_1(tr)J_1(ta)$$

$$\times [e^{-tz} - e^{-t(h-z)}]dt, \quad |r| \le a. \qquad (8)$$

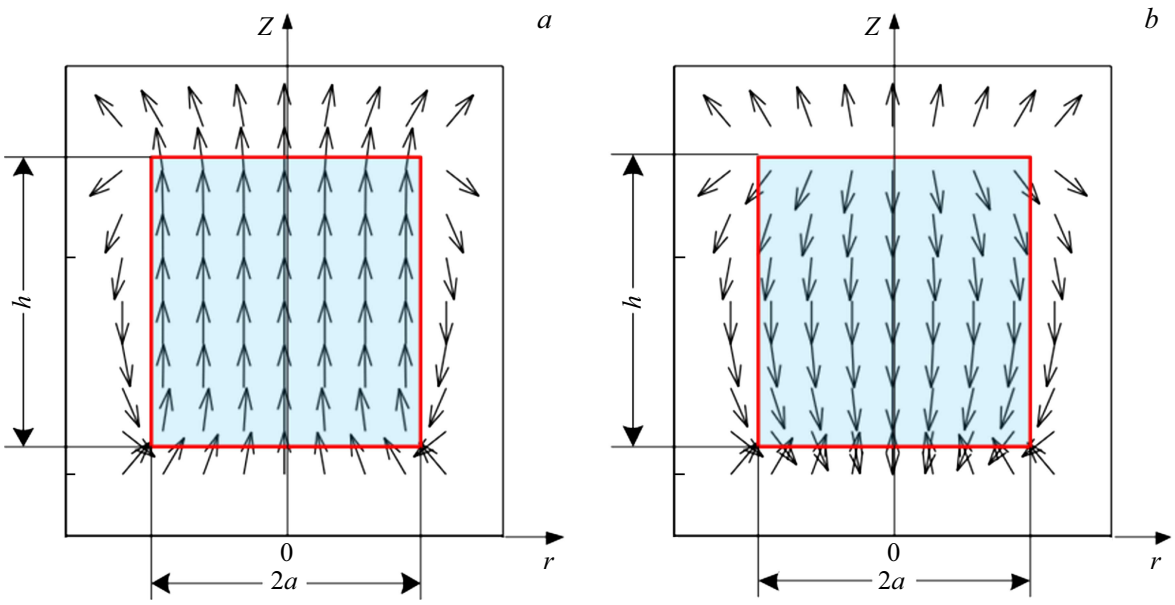

Figure 2. *a* — vector field of induction **B**. The induction lines are continuous; *b* — vector field $\mathbf{H}_p$. The $\mathbf{H}_p$ field suffers rupture at the ends of the cylinder. The demagnetizing field $\mathbf{H}_p$ in the volume of the cylinder is directed opposite to the magnetization $\mathbf{M}_z$. Outside the cylinder, the field and induction lines coincide.

Formulas for calculating the 3*D* coefficients $N_{zz}(r,z)$ and $N_{rz}(r,z)$ in the entire space have the form

$$N_{zz}(r,z) =$$
$$\begin{cases} \frac{1}{2}a\int_0^\infty J_0(tr)J_1(ta)[e^{-tz}+e^{-t(h-z)}]dt, & \text{if } (0\le z\le h),\\ \frac{1}{2}a\int_0^\infty J_0(tr)J_1(ta)[e^{-tz}-e^{t(h-z)}]dt, & \text{if } (z>h),\\ \frac{1}{2}a\int_0^\infty J_0(tr)J_1(ta)[e^{-t(h-z)}-e^{tz}]dt, & \text{if } (z<0),\\ -\frac{1}{2}\left[\frac{h-z}{\sqrt{(h-z)^2}}+\frac{z}{\sqrt{z^2+a^2}}-\frac{h-z}{|h-z|}-\frac{z}{|z|}\right] & \text{everywhere,} \end{cases} \tag{9}$$

$$N_{rz}(r,z) =$$
$$\begin{cases} \frac{1}{2}a\int_0^\infty J_1(tr)J_1(ta)[e^{-tz}-e^{-t(h-z)}]dt, & \text{if } (0\le z\le h),\\ \frac{1}{2}a\int_0^\infty J_1(tr)J_1(ta)[e^{-tz}-e^{t(h-z)}]dt, & \text{if } (z>h),\\ \frac{1}{2}a\int_0^\infty J_1(tr)J_1(ta)[e^{tz}-e^{-t(h-z)}]dt, & \text{if } (z<0). \end{cases} \tag{10}$$

Cylinder induction

$$B_z(r,z) = \mu_0(H_p + M_z) = \mu_0 M_z(1 - N_{zz}).$$

Taking into account *z*- and *r*-field components and cylinder induction

$$H_z(r,z) = -M_z\, N_{zz}(r,z), \tag{11}$$

$$H_r(r,z) = -M_z\, n_{rz}(r,z). \tag{12}$$

$$B_z(r,z) =$$
$$\begin{cases} \mu_0 M_z(1-N_{zz}) & \text{if } (0\le z\le h)\wedge(0\le|r|\le a),\\ \mu_0 H_z(r,z) & \text{everywhere,} \end{cases} \tag{13}$$

$$B_r(r,z) = \mu_0 H_r(r,z). \tag{14}$$

Evaluation by formulas (9), (10) directly near the sample surface lead to oscillating solutions [27]. In [28,29] N_{zz} and N_{rz} were redefined in terms of elliptic integrals Calculation of stray fields through elliptic integrals provides stable numerical results for any parameters of the magnetic system. These formulas, written for characteristic areas inside and outside the cylinder, are given in the Appendix [30].

Fig. 2 shows graphs of the vector fields of induction $\mathbf{B}_{cyl}$ and the cylinder fields $\mathbf{H}_p$ in a form normalized to the absolute value of the vectors. The shaded area indicates the axial section of the cylinder. The graphs are plotted for a cylinder of size $h = 50$ cm, $2a = 10$

Fig. 3 shows graphs of changes in the demagnetizing field H_p and induction B_z along the axis *Z* for the following parameter $h = 50$ cm, $2a = 10$ cm, $M_z = 5\cdot10^3$ A/m.

Fields and induction in the *X*–*Y* plane (Fig. 1) are calculated as follows:

$$H_z(x,y) = H_r(r,z)q(x,z),\ \ H_y(x,y) = H_r(r,z)g(x,z),$$

$$H_z(x,y) = H_z(r,z),$$

$$B_z(x,y) = B_r(r,z)q(x,z),\quad B_y(x,y) = B_r(r,z)g(x,z),$$

$$B_z(x,y) = B_z(r,z),$$

where

$$r(x,y) = \sqrt{x^2+y^2}, \quad q(x,y) = \frac{x}{\sqrt{x^2+y^2}},$$

$$g(x,y) = \frac{y}{\sqrt{x^2+y^2}}.$$

2. Cylinder energy. Volume-average demagnetizing factor as Nagaoka coefficient

The energy of the cylinder is given by the formula

$$E_{cyl}(a,h) = 2\pi \int_0^h \int_0^a \frac{M_z B_z(r,z)}{2} r dr\, dz$$

$$= 2\pi \int_0^h \int_0^a \frac{\mu_0 M_z^2 [1 - N_{zz}(r,z)]}{2} r dr\, dz. \quad (15)$$

The induction component $B_r(r,z)$is perpendicular to $M_z$and does not contribute to the energy. With the introduction of a volume-averaged demagnetizing factor of the cylinder

$$\bar{N}_z(a,h) = \frac{2\pi}{\pi a^2 h} \int_0^h \int_0^a N_{zz}(r,z) dr\, dz, \quad (16)$$

$E_{cyl}(a,h)$ can be represented in equivalent form

$$E_{cyl}(a,h) = 2\pi \int_0^h \int_0^a \frac{\mu_0 M_z^2 [1 - \bar{N}_z(r,z)]}{2} r dr\, dz$$

$$= E_0(a,h) - E_p(a,h), \quad (17)$$

where E_0 — the energy of a section length h of an infinite long cylinder, E_p — the energy of the demagnetizing field.

The equality of energies E_{coil} (2) and $E_{cyl}(a,h)$ (17) establishes a connection between the Nagaoka coefficient k_L (3) and the coefficient $k1_L$ determined by (16):

$$k1_L = 1 - \bar{N}_z(a,h). \quad (18)$$

The term „cylinder inductance“ has no physical meaning. However, taking into account the equality of the energies of the cylinder and the coil $E_{cyl}(a,h) = E_{coil}(a,h)$ from the energy $E_{cyl}(a,h)$ taking into account (4) it is possible to calculate from (2) the inductance of the equivalent coil $L = 2E_{cyl}/I^2$. For cylinder and coil parameters: $h = 50$ cm, $a = 5$ cm, $I = 5$ A, $w = 500$, $j = 5 \cdot 10^3$ A/m, $M_z = 5 \cdot 10^3$ A/m we obtain $E_{cyl}(a,h) = 0.057$ J, $E_p(a,h) = 4.929 \cdot 10^{-3}$ J, $E_0(a,h) = 0.062$ J, $\bar{N}_z(a,h) = 0.08$, $k_L = k1_L = 0.92$, $L = 4.64 \cdot 10^{-3}$ H.

Fig. 4 shows graphs of the dependence of the coefficients k_L and $k1_L$ on the lengths of the coil and cylinder in the range $h = 0-100$ cm

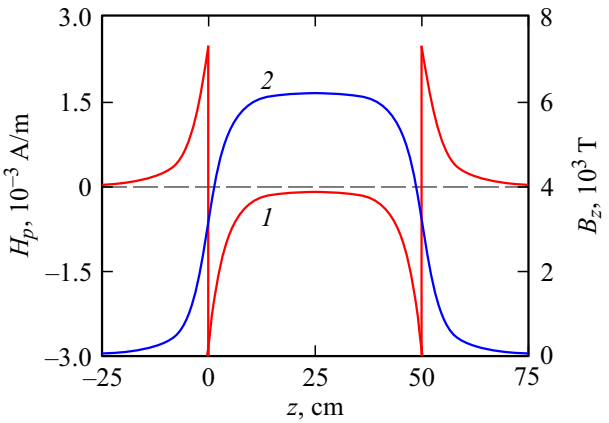

Figure 3. *1* — demagnetizing field H_p; *2* — induction B_z, $r = 0.1$ cm, $z = -25-75$ cm.

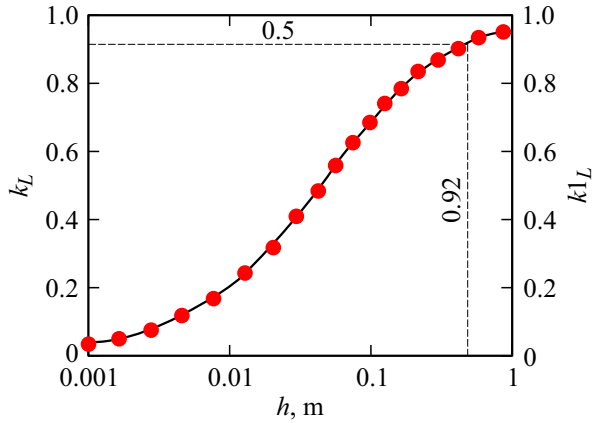

Figure 4. Solid line k_L — Nagaoka coefficient in Lorentz form. Symbolic line — $k1_L$, determined by the demagnetizing factor of the cylinder, $h = 0-100$ cm.

3. Criterion„short coil“ [31]

Currently there is no generally accepted definition of coils based on the h/a ratio criterion. The definitions range from „long“ $h > 2a$to „very short“ $2a \ll h$. Below we propose a definition of a short coil based on the ratio of volumetric energy densities $\bar{E}_{syl} = E_{syl}/h\pi a^2$ [J/m^3 of an equivalent cylinder (17).

Fig. 5 shows the dependences of the h, $\bar{E}_p(a,h)$ of volumetric energy densities and the demagnetizing factor $\bar{N}_z(a,h)$.

It follows from the graphs that the energy „of the long“ cylinder $(h \gg 2a)$ $\bar{E}_{cyl}(a,h)$ — curve *1* — dominates. However, as h decreases, starting from a certain value of h_{kr}, in this case $h \le 4.5$ cm, the demagnetization energy $\bar{E}_p(a,h)$ — curve *2* prevails. This effect occurs at $\bar{N}_z \le 0.5$ $(n \le 4.5$ cm) — curve *3*. The value h_k depends on the ratio $2a/h$, but at the same time the value of I$\bar{N}_z(a,h) = 0.5$ does not change and it can be proposed as a criterion for a short coil. This result does not follow from the current model.

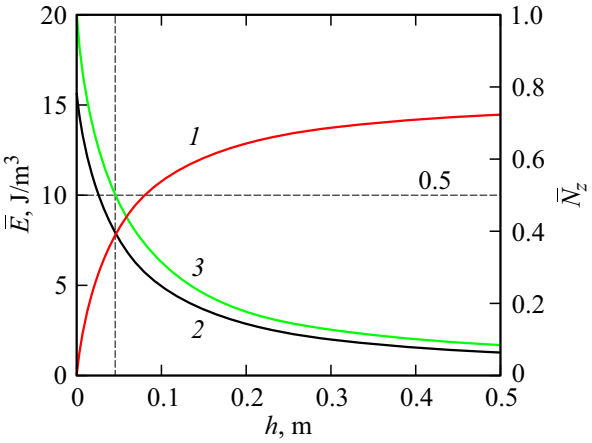

Figure 5. Change in volumetric energy densities and the average demagnetizing factor over the volume of the cylinder in the range of changes in the length of the cylinder, $z = 0-50$ cm, *1* — energy of the cylinder $\bar{E}_{cyl}$; *2* — demagnetizing field energy $\bar{E}_p$; *3* — average demagnetizing factor over the volume of the cylinder $\bar{N}_z$, $\bar{N}_z = 0.5$ at $h = 4.5$ cm.

4. Ponderomotive forces in axisymmetric systems

4.1. Surface radial and axial forces. Thiele's strength function

Taking into account the equality of the internal energies of the cylinder and coil, further, unless otherwise stated, the terms „cylinder" and „coil" will be considered equivalent. Radial F_r and axial F_z forces are determined from the derivatives of energy $E_{cyl}(a, h)$ (17) along the coordinates r and z

$$F_r(a, h) = -\frac{d}{da} E_{cyl}(a, h), \quad F_z(a, h) = -\frac{d}{dh} E_{cyl}(a, h).$$

For the parameters $h = 50$ cm, $2a = 10$ cm, $M_z = 5 \cdot 10^3$ A/m we have $F_r(a, h) = -2.178$ N, $F_z(a, h) = -0.123$ N, which coincides with the calculations of the forces for the coil ($w = 500$, $I = 5 \cdot$ A).

Radial forces tend to increase the diameter of the magnetic system, and axial forces lead to compression of the system at the ends. For coils, the occurrence of such forces follows from Ampere's law [32]. These effects for both the coil and the cylinder follow from the law of conservation of energy. The volumetric-averaged energy density of the system $\bar{E} = E/h\pi a^2$, where E is defined (17), decreases with increasing $2a$, which leads to the emergence of forces tending to increase the diameter of the cylinder. With an increase in h , $\bar{E}$ grows too, which causes the occurrence of compressive axial end stresses.

The mathematical expression for the radial force $F_r(a, h)$ is equivalent to the equation for F expressed through the Thiele force function $F(r, h)$ introduced in the theory of stability of cylindrical magnetic domains (CMD) [33]:

$$F(r, h) = \frac{2}{\pi}\left(\frac{2r}{h}\right)^2\left[\frac{1}{r(r, h)} Ec(r, h) - 1\right],$$

$$Ec(r, h) \int_0^{\pi/2} \sqrt{1 - k(r, h)^2 \sin^2\theta} d\theta, \quad k(r, h) = \sqrt{\frac{4r^2}{4r^2 + h^2}}$$

and $F_r(r, h) = \mu_0/2\pi h^2 M_z^2 F(r, h)$, where$r$ -is the radius of the CMD, h — the thickness of the infinite plate containing the domain, M_z — the magnetization of the isolated CMD (without taking into account the magnetization of the plate). In [{]34for a quick estimate of $F_r(r, h)$, a simple interpolation expression $F_r(r, h) = 4r/(2h + 3r)$ is proposed. In the range $(0 \le 2r/h \le 10)$ the formula is valid with an accuracy of several percent.

4.2. Radial and axial stresses in multilayer systems

The calculation diagram for ponderomotive forces for a system of three coaxial cylinders $n = 3$ is shown in Fig. 6 [35]. Further, in the formulas for the lengths of the cylinders, the designation L_n is introduced, and the origin of coordinates is moved to the center of the magnetic system by replacing $z' = z + L_n/2$, which ensures the symmetry of the graphs relative to the origin of coordinates.

Further, the following notations are introduced in the calculation formulas: M — number of layers of coils (cylinders), n — serial number of the layer $(n = 1 \ldots M)$, w_n — number of turns of$n$-th coil layer, $2a_1$ — — diameter of n-th layer, $2a_M$ — diameter of the outer layer.

To demonstrate the model, the calculations assumed equal magnetizations and lengths of concentric cylinders with the number of layers $M = 3$. To set the distance between layers according to r a power function was selected: $Funck(a_M, a_1, n, k) = [(n - 1/M - 1)^k](a_M - a_1)$,

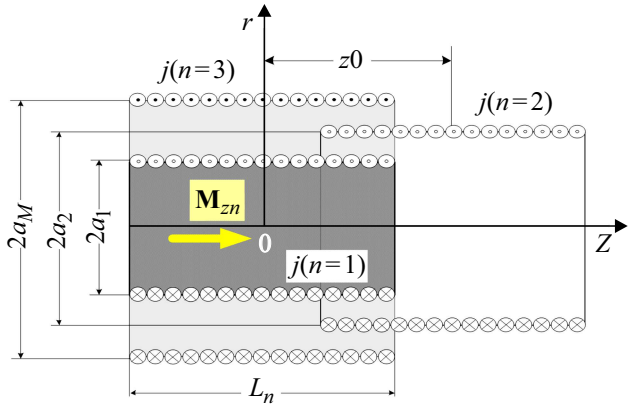

Figure 6. Calculation diagram of ponderomotive forces for a system of three cylinders (coils) $n = 3$. $M_z(n)$ — magnetization of the n-th layer of the cylinder z_0 — shift n-th cylinder relative to the origin, $j(n)$ — surface current density n-th cylinder (coil).

where k — exponent; $k = 1$ corresponds to equal distances between layers. The radius of the$n$-th layer is defined as

$$a_n = \begin{cases} a_1, \text{ if } n = 1 \vee M = 1, \\ \text{no value if } n > M, \\ a_1 + Funck(a_M, a_1, n, k) \text{ everywhere.} \end{cases}$$

Below the calculation results are presented for the following system parameters:

$$a_n = \begin{cases} 10\,\text{cm}, \ n = 1, \\ 15\,\text{cm}, \ n = 2, L_n = 20\,\text{cm}, w_n = 100, \\ M_{zn} = 21.5 \cdot 10^3\,\text{A/m}, I_n = 5\,\text{A/turn}\,(n = 1, 2, 3), \\ 20\,\text{cm}, \ n = 3. \end{cases}$$

The energy of the selected cylinder in the fields of the other two at $z0 = 0$ is equal to the sum of the mutual energies. Thus, the energy of the$n$-th concentric cylinder in the i-th and j-th fields is written in the form

$$E_{nij}(L_n, a_n) = 2\pi \times \int_{-L_n/2}^{L_n/2} \int_0^{a_n} \frac{M_{zn}[B_{zi}(M_i, L_i, a_i) + B_{zj}(M_j, L_j, a_j)]}{2} r dr\, dz = E_{ni} + E_{nj}, \ n, i, j = 1, 2, 3, \quad (19)$$

where $E_{ni} + E_{nj}$ — mutual energies of the cylinders.

Radial and axial forces are calculated from (19) using the formulas

$$F_{rnij} = \frac{d}{da_n}[E_{ni}(L_i, a_i) + E_{nj}(L_j, a_j)], \quad (20)$$

$$F_{znij} = \frac{d}{dL_n}[E_{ni}(L_i, a_i) + E_{nj}(L_j, a_j)]. \quad (21)$$

Totally normalized to the surface areas, the radial $\langle\sigma_{rnij}\rangle$ and axial $\langle\sigma_{znij}\rangle$ mechanical stresses N/m^2) of the n-th cylinder in the fields of i-th one and j-th one are defined as

$$\langle\sigma_{rnij}\rangle = \frac{d}{da_n}\left[\frac{E_{ni}(L_i, a_i)+E_{nj}(L_j, a_j)}{L_n 2\pi a_n}\right] = \langle\sigma_{rni}\rangle+\langle\sigma_{rnj}\rangle, \quad (22)$$

$$\langle\sigma_{znij}\rangle = \frac{d}{dL_n}\left[\frac{E_{ni}(L_i, a_i)+E_{nj}(L_j, a_j)}{\pi a_n^2}\right] = \langle\sigma_{zni}\rangle+\langle\sigma_{znj}\rangle. \quad (23)$$

The mutual energies of the cylinders are equal in pairs. The equality of mutual energies does not mean the equality of mutual surface stresses, which is explained by the different surface areas of the cylinders due to the difference in their diameters.

With $(n = i = j)$, the internal voltage of the cylinder n-th is obtained (15). Radial $\langle\sigma_{rn}\rangle$ and axial $\langle\sigma_{zn}\rangle$ force densities along the cylindrical and end surfaces of the n-th in the own field B_{zn} are equal

$$\langle\sigma_{rn}\rangle = \frac{d}{da_n} E_n(L_n, a_n)/L_n 2\pi a_n,$$

$$\langle\sigma_{zn}\rangle = \frac{d}{dL_n} E_n(L_n, a_n)/\pi a_n^2. \quad (24)$$

For an isolated cylinder at $L_n \to \infty$ we have the equality $\langle\sigma_z\rangle = \langle\sigma_z\rangle$ [31,32].

Fig 7 shows the mutual radial mechanical stresses along the generatrices of three cylinders in pairs.

Arrow lengths are shown to scale. The resulting radial stresses acting on an individual cylinder are obtained (taking into account the sign) by summing the stresses according to the diagram shown in the figure. So, $\langle\sigma_{r132}\rangle = \langle\sigma_{r13}\rangle + \langle\sigma_{r12}\rangle = 4.06$, which corresponds to calculations using formula (22).

The energy of the system of coaxial displaced cylinder of n-th is by a distance $z0$ in the Z-direction in the fields of cylinder i-th and j-th one is equal

$$E_{nij}(L_n, a_n, z0) = 2\pi \times \int_{-L_n/2}^{L_n/2} \int_0^{a_n} \frac{M_{zn}[B_{zi}(z - z0)B_{zj}(z - z0)]}{2} r dr\, dz = E_{ni} + E_{nj}. \quad (25)$$

Longitudinal (axial) forces $F_{znij}(Z0)$ and mechanical stresses $\langle\sigma_{rnij}\rangle$ when the n-th cylinder is displaced in the Z-direction (Fig. 6) in the fields of the i-th and j -th cylinders are calculated by the formulas

$$F_{znij}(z0) = dE_{nij}(L_n, a_n, z0)/da_n,$$

$$\langle\sigma_{znij}\rangle = F_{znij}(z0)/\pi a_n^2. \quad (26)$$

Radial forces and stresses are determined similarly

$$F_{rnij}(z0) = dE_{nij}(L_n, a_n, z0)/dL_n,$$

$$\langle\sigma_{rnij}\rangle = F_{znij}(z0)/L_n 2\pi a_n. \quad (27)$$

For a cylinder system, the resulting forces and stresses are obtained by simple summation. The results of stress calculations not included in this work are given in [31,35].

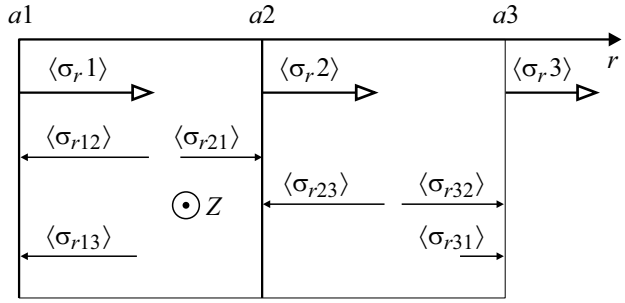

Figure 7. Surface radial stresses of cylinders. $\langle\sigma, 1\rangle$, $\langle\sigma, 2\rangle$, $\langle\sigma, 3\rangle$ — stresses acting on the cylindrical surfaces of individual cylinders in their own fields (N/m^2). $\langle\sigma, 1\rangle = 2.275$, $\langle\sigma, 2\rangle = 1.867$, $\langle\sigma, 3\rangle = 1.588$. Mutual stresses $\langle\sigma_{r12}\rangle = 2.275$, $\langle\sigma_{r21}\rangle = 1.43$, $\langle\sigma_{r23}\rangle = 2.078$, $\langle\sigma_{r32}\rangle = 1.767$, $\langle\sigma_{r13}\rangle = 1.801$, $\langle\sigma_{r31}\rangle = 0.818$ [35].

Parameters of the magnetic system$n = 3$ ($z0 = 0$) [35]

Radius and number cylinder a_n, cm	Energy cylinder E_n, J	Radial voltage cylinder, $\langle\sigma_r\rangle$, N/m^2	Axial voltage cylinder, $\langle\sigma_z\rangle$, N/m^2	Reciprocal energy cylinders E_{ni}, J	Reciprocal radial tension, $\langle\sigma_{rnij}\rangle$, N/m^2	Inductance coils, L_n, 10^3 H	Reciprocal inductance coils, M_{ni}, 10^3 H
$a_1 = 10$	0.017	−2.276	−3.406	$E_{12} = 0.013$	$\langle\sigma, 3_{12}\rangle = -2.585$	$L_1 = 1.359$	$M_{12} = 1.058$
$a_2 = 15$	0.033	−1.867	−3.013	$E_{13} = 0.011$	$\langle\sigma, 2_{13}\rangle = -3.509$	$L_2 = 2.643$	$M_{13} = 0.86$
$a_3 = 20$	0.052	−1.588	−2.714	$E_{23} = 0.026$	$\langle\sigma, 1_{23}\rangle = -4.06$	$L_3 = 4.149$	$M_{23} = 2.075$

5. Mutual inductance of coaxial coils [30]

Below a diagram for calculating mutual inductance in a system of three coaxial coils ($n = 3$) (Fig. 1) is given. Calculations were performed for the input parameters introduced in Section 4.2.

The essence of the method is to calculate the mutual energy between pairs of cylinders. Calculating the energy and mutual energy of the cylinders is the most important intermediate step in calculating the mutual inductance of the coils. The energy of the$n$-th cylinder with radius a_n in the field of the i-th with radiusa_i is determined by (19). The self ($n = i$) and mutual inductances of the coils are calculated from the energies and mutual energies of the cylinders [36]:

$$M_{ni} = \frac{2E_{cyl}(n, i)}{I_n I_i}. \qquad (28)$$

Taking into account the equality of the mutual energies of the cylinders, it is sufficient to perform M_{ni}calculations only for one pair of the system. The energy of n-th cylinder and the self-inductance n of the Lth coil are calculated using formulas (2), (19), (30), if we give in the latter$n = i$. Paired mutual inductances, i.e. inductance N of connected

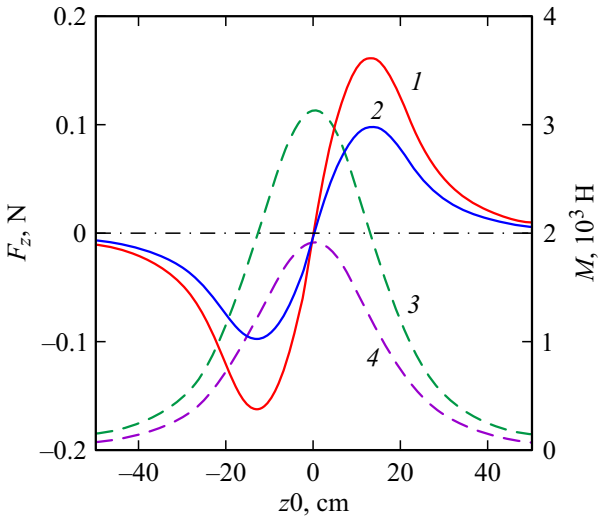

Figure 8. Forces F_z and mutual inductances M. *1* — $F_{z\,213}(n = 2)$, *2* — $F_{z\,123}(n = 1)$, *3* — $M_{213}(n = 2)$, *4* — $M_{123}(n = 1)$.

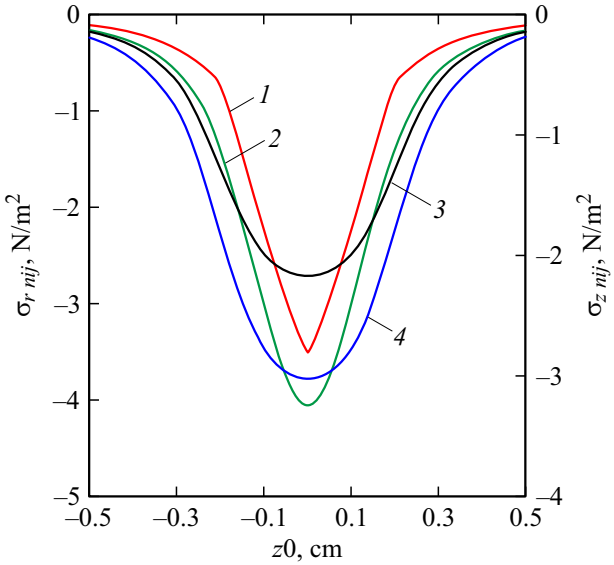

Figure 9. Surface radial stresses $\langle\sigma_r\rangle$ and axial stresses $\langle\sigma_z\rangle$. *1* — $\sigma_{r\,213}(n = 2)$, *2* — $\sigma_{r\,123}(n = 1)$, *3* — $\sigma_{z\,213}(n = 2)$, *4* — $\sigma_{z\,123}(n = 1)$. $z = -0.5$–0.5 m.

circuits, determined from energies, are calculated using known formulas [37].

The given general method for calculating energies was applied in [27,30,31] to calculate longitudinal ponderomotive forces, mutual inductance of the coil system and surface mechanical stresses. All calculated values correspond to the data of the work [11].

The results of calculations of the parameters of magnetic systems for $n = 3$ are summarized in the table. The notation $\langle\sigma_r n_{ij}\rangle$ means the radial stresses acting on the In–th layer of the cylinder (coil) in the fields of the i-th and jth layers.

Fig. 8 shows graphs of axial forces F_z acting on the n- th in the cylinder's fields i-th and j-th when it is displaced in the Z direction relative to the origin by a distance $z0$ and the corresponding mutual inductances M equivalent coils (Fig. 6).

Fig. 9 illustrates the change in surface radial $\langle\sigma_{rnij}\rangle$ and axial mechanical stresses $\langle\sigma_{znij}\rangle$ when the n-th cylinder is displaced in the Z-direction (Fig. 6) in the fields of the i-th and j-th cylinders.

6. Inductance of a rectangular coil

Inductance is calculated from the energy of a straight hollow axially magnetized cylinder (torus) with winding thickness t. The energy is equal to the difference between the energies of cylinders with radii $a + t/2$ and $a - t/2$, defined by (17). The cylinders have opposite directions of magnetization M_z. According to (18), this energy is the energy of the equivalent coil:

$$E_t(a, t, L) = 2\pi \int_{-L/2}^{L/2} \int_{a-t/2}^{a+t/2} \frac{M_z B_z(a, t, L)}{2} r dr\, dz. \quad (29)$$

For a coil with a radius along the middle turn $a = 5\,\text{cm}$, length $L = 20\,\text{cm}$, $w = 500$ winding thickness $t = 2\,\text{cm}$ and current in the turn $I = 5\,\text{A}$ ($M_z = 1.25 \cdot 10^4\,\text{A/m}$) energy $E_t(a, t, L) = 0.108\,\text{J}$. Coil inductance$L_t = 2E_t/I^2 = 8.621 \cdot 10^{-3}\,\text{H}$. The inductance of the coil along the middle $L_{mid} = 10.095 \cdot 10^{-3}\,\text{H}$. Correction for winding thickness $\Delta L = 1.472 \cdot 10^{-3}\,\text{H}$) The results are consistent with the data given in example 6−7 [11].

Conclusion

The work shows the advantages of the presented method for calculating multicomponent axial axisymmetric systems in terms of simplicity and versatility. In terms of calculations of ponderomotive forces, the method is applicable both to current axisymmetric coils and to magnetic cylinders. The presented numerical results correspond to the values of the parameters given in [11], from which the input parameters of a number of test calculations were borrowed. Compliance with models of other authors has been established. Calculations of systems with parallel and non-coinciding axes are possible. These calculations are not conceptually new and are not presented in the work. In any case, the energy of the selected cylinder or its part (torus) in the fields of other elements of the system is calculated. The model does not impose any restrictions on the relative arrangement of the elements of the system being calculated, or on their geometric and magnetic parameters.

Radial and axial forces (voltages) acting on the surface of the cylinder (coil) are calculated from the energy stored in the magnetic field of the cylinder, bypassing the stage of calculating the inductance. The independence of demagnetizing coefficients from external fields allows the use of the energy approach to calculate complex systems composed of individual elements, for example, cylinders, coils and/or rectangular prisms.

Conflict of interest

The author declares that he has no conflict of interest.

Appendix

Demagnetizing factors and 3D-fields of the cylinder, expressed through elliptic integrals [30]

Demagnetization coefficients (9), (10) can be written through elliptic integrals

$$N_z(r, z) = 4\pi\left[1 - \frac{z k_1 Kc(k_1)}{4\pi\sqrt{ar}} - \frac{\Lambda_0(\alpha_1, \beta_1)}{4} - \frac{(L - z)k_2 Kc(k_2)}{4\pi\sqrt{ar}} - \frac{\Lambda_0(\alpha_2, \beta_2)}{4}\right], \quad (A1)$$

$$N_{rz}(r, z) = 4\pi\left(\frac{1}{\pi}\right)\sqrt{\frac{a}{r}}\left\{\left(\frac{1}{k_1}\right)\left[\left(1 - \frac{k_1^2}{2}\right)Kc(k_1) - Ec(k_1)\right] - \left(\frac{1}{k_2}\right)\left[\left(1 - \frac{k_2^2}{2}\right)Kc(k_2) - Ec(k_2)\right]\right\}, \quad (A2)$$

where $\Lambda_0(\alpha, \beta)$ — Heyman's lambda function — complete elliptic integral of the third kind; $\Lambda_0(\alpha, \beta)$ is expressed through complete $Kc(k), Ec(k)$ and incomplete $F(\beta, k), E(\beta, k)$ elliptic integrals of the 1st and 2nd kind [37].

$$\Lambda_0(\alpha_1, \beta_1) = \left(\frac{2}{\pi}\right)\left[E_c(k_1)F\left(\beta_1, \sqrt{1 - k_1^2}\right) + K_c(k_1)E\left(\beta_1, \sqrt{1 - k_1^2}\right) - K_c(k_1)F\left(\beta_1, \sqrt{1 - k_1^2}\right)\right],$$

$$\Lambda_0(\alpha_2, \beta_2) = \left(\frac{2}{\pi}\right)\left[E_c(k_2)F\left(\beta_2, \sqrt{1 - k_2^2}\right) + K_c(k_2)E\left(\beta_2, \sqrt{1 - k_2^2}\right) - K_c(k_2)F\left(\beta_2, \sqrt{1 - k_2^2}\right)\right],$$

integrals

$$K_c(k) = \int_0^{\pi/2} (1 - k^2 \sin^2\theta)^{1/2} d\theta$$

and

$$E_c(k) = \int_0^{\pi/2} \sqrt{1 - k^2 \sin^2\theta}\, d\theta.$$

Modules $K_c(k)$, $E_c(k)$ are equal

$$k_1^2 = 4ar[z^2 + (a + r)^2]^{-1},\ k_2^2 = 4ar[(h - z)^2 + (a + r)^2]^{-1}.$$

Incomplete integrals $F(\beta, k), E(\beta, k)$ with additional modules m and amplitudes β are written in the form

$$F(\beta, m) = \int_0^{\beta} \frac{1}{\sqrt{1 - m^2 \sin^2\theta}}\, d\theta,$$

$$E(\beta, m) = \int_0^{\beta} \sqrt{1 - m^2 \sin^2\theta} d\theta,\ m_1 = \sqrt{1 - k_1^2},$$

$$m_2 = \sqrt{1 - k_2^2},\ \alpha_1 = \arcsin k_1,\ \alpha_2 = \arcsin k_2,$$

$$\beta_1 = \arcsin \frac{z}{\sqrt{z^2 + (a - r)^2}},$$

$$\beta_2 = \arcsin \frac{h - z}{\sqrt{(h - z)^2 + (a - r)^2}},$$

where $\alpha_1, \alpha_2, \beta_1, \beta_2$ are main arcsin values.

Formulas (A1), (A2) determine the demagnetizing factors N_{zz} and N_{rz} in the volume of the cylinder. When calculating fields outside the cylindrical region, it is necessary to redefine the calculation formulas. Below are the relations for the coefficients N_{zz} and N_{rz}, which allow one to calculate the fields and induction of the cylinder in the entire space. Formulas are written separately for characteristic areas inside and outside the cylinder, determined by the ranges of change z and r [30]:

$$N_{zz}(r, z) =$$
$$\begin{cases} \text{if } (0 \le z \le h) \wedge (|r| \le a) \\ \left[1 - \frac{z k_1 K_c(k_1)}{4\pi\sqrt{ar}} - \frac{\Lambda_0(\alpha_1, \beta_1)}{4} - \frac{(h-z) k_2 K_c(k_2)}{4\pi\sqrt{ar}} - \frac{\Lambda_0(\alpha_2, \beta_2)}{4}\right] \\ 0 \text{ if } (0 \le z \le h) \wedge (r = 0) \\ -\frac{z k_1 K_c(k_1)}{4\pi\sqrt{ar}} + \frac{\Lambda_0(\alpha_1, \beta_1)}{4} - \frac{(h-z) k_2 K_c(k_2)}{4\pi\sqrt{ar}} - \frac{\Lambda_0(\alpha_2, \beta_2)}{4} \\ \text{if } (z < 0) \wedge (0 < |r|) < a \\ -\frac{z k_1 K_c(k_1)}{4\pi\sqrt{ar}} - \frac{\Lambda_0(\alpha_1, \beta_1)}{4} - \frac{(h-z) k_2 K_c(k_2)}{4\pi\sqrt{ar}} + \frac{\Lambda_0(\alpha_2, \beta_2)}{4} \\ \text{if } (z > h) \wedge (0 < |r|) < a \\ -\frac{z k_1 K_c(k_1)}{4\pi\sqrt{ar}} + \frac{\Lambda_0(\alpha_1, \beta_1)}{4} - \frac{(h-z) k_2 K_c(k_2)}{4\pi\sqrt{ar}} + \frac{\Lambda_0(\alpha_2, \beta_2)}{4} \\ \text{if } (0 < z < h) \wedge (|r| > a) \\ -\frac{z k_1 K_c(k_1)}{4\pi\sqrt{ar}} - \frac{\Lambda_0(\alpha_1, \beta_1)}{4} - \frac{(h-z) k_2 K_c(k_2)}{4\pi\sqrt{ar}} + \frac{\Lambda_0(\alpha_2, \beta_2)}{4} \\ \text{if } (z < 0) \wedge (|r| \ge a) \\ -\frac{z_1 k_1 K_c(k_1)}{4\pi\sqrt{ar}} + \frac{\Lambda_0(\alpha_1, \beta_1)}{4} - \frac{(h-z) k_2 K_c(k_2)}{4\pi\sqrt{ar}} - \frac{\Lambda_0(\alpha_2, \beta_2)}{4} \\ \text{if } (z > h) \wedge (|r| \ge a) \\ -\frac{1}{2}\left[\frac{h - z}{\sqrt{(h-z)^2 + a^2}} + \frac{z}{\sqrt{z^2 + a^2}} - \frac{h - z}{|h - z|} - \frac{z}{|z|}\right] \\ \text{if } r = 0 \\ 0 \text{ everywhere,} \end{cases} \tag{A3}$$

$$N_{rz}(r, z) =$$
$$\begin{cases} \left(\frac{1}{\pi}\right)\left(\sqrt{\frac{a}{r}}\right)\left\{\left(\frac{1}{k_1}\right)\left[\left(1 - \frac{k_1^2}{2}\right)K_c(k_1) - E_c(k_1)\right]\right. \\ \left. - \left(\frac{1}{k_2}\right)\left[\left(1 - \frac{k_2^2}{2}\right)K_c(k_2) - E_c(k_2)\right]\right\} \text{ if } r > 0 \\ - \left(\frac{1}{\pi}\right)\left(\sqrt{\frac{a}{r}}\right)\left\{\left(\frac{1}{k_1}\right)\left[\left(1 - \frac{k_1^2}{2}\right)K_c(k_1) - E_c(k_1)\right]\right. \\ \left. - \left(\frac{1}{k_2}\right)\left[\left(1 - \frac{k_2^2}{2}\right)K_c(k_2) - E_c(k_2)\right]\right\} \text{ if } r < 0 \\ 0 \text{ everywhere.} \end{cases} \tag{A4}$$

The last formula (line) in (PC) is written for the demagnetizing factor on the axis.

Conflict of interest

The author declares that he has no conflict of interest.

References

[1] D.B. Montgomeri. *Solenoid Magnet Design* (Wiley-Interscience, NY., 1971)

[2] V.R. Karasik. *Fizika i tekhnika sil'nykh magnitnykh poley* (Nauka, M., 1964) (in Russian)

[3] H. Knoepfel. *Pulsed High Magnetic Fields* (North-Holland, Amsterdam 1970)

[4] D.H. Parkinson, B.E. Mulhall. *The Generation of High Magnetic Fields* (Plenum Press, NY., 1967)

[5] B.L. Alievsky, A.M. Oktyabrsky, V.L. Orlov, V.A. Postnikov. *Modeling of magnetic fields of axisymmetric systems*: textbook. manual, ed. B.L. Alievsky (MAI Publishing House, M., 2007) (in Russian)

[6] A.S. Lagutin, V.I. Ozhogin. *Sil'nyye impul'snyye magnitnyye polya v fizicheskom eksperimente* (Energoatomizdat, M., 1988) (in Russian)

[7] Electronic media. Available at: http://coil32.ru/, http://electronbunker.ca, http://g3ynh.info/zdocs/magnetics/

[8] J.C. Maxwell. *A Treatise on Electricity and Magnetism* (Dover Publ., NY., 1954), v. 2.

[9] L. Lorenz. *Über die Fortpflanzung der Elektrizität* (Annalen der Physik, **VII**, 1879)

[10] H. Nagaoka. J. College Science, **27**, 18 (1909).

[11] P.L. Kalantarov, L.A. Tseytlin. *Raschet induktivnostey* (Energoatomizdat, L., 1986) (in Russian)
M.V. Nemtsov. *Spravochnik po raschetu parametrov katushek induktivnosti* (Energoatomizdat, M., 1989) (in Russian)

[13] G.A. Shtamberger. *Ustroystva dlya sozdaniya slabykh postoyannykh magnitnykh poley*, ed. K.B. Karandeyeva (Nauka, Novosibirsk, 1972) (in Russian)

[14] R.J. Joseph, J. Schlömann. Appl. Phys., **36** (5), 1579 (1964).

[15] A.K. Andreev. *State Registration Certificate of Computer* (Program N 2012614673, Byull. Izobret., No. 3, (2012), part 2, p. 378)

[16] T. Taniguchi. J. Magn. Magn. Mater., **452**, 464 (2018). DOI: 10.1016/j.jmmm.2017.11.078

[17] A. Caciagli, R.J. Baars, A.P. Philipse, B.W.M. Kuipers. J. Magn. Magn. Mater., **456**, 423 (2018). DOI: 10.1016/j.jmmm.2018.02.003
[18] R. Ravaud, G. Lemarquand, V. Lemarquand, S. Babic, C. Akyel. PIER, **102**, 367 (2010). DOI: 10.2528/PIER07101504
[19] J. Conway. IEEE Trans. Magn., **43** (3), 1023 (2007). DOI: 10.1109/TMAG.2006.888565
[20] S. Babic, C. Akyel. Physics, **2** (3), 352 (2020). DOI: 10.3390/physics2030019
[21] L.B. Luganskiy. Elektrichestvo, **2**, 55 (2017) (in Russian).
[22] A.K. Andreev. J. Mach. Manuf. Reliab, **48** (1), 26 (2019). DOI: 10.3103/S1052618819010035
[23] E. Pursell. *Electricity and Magnetism* (Cambridge Univ. Press, Cambridge, 2013)
[24] A.I. Akhiezer, V.G. Bar'yakhtar, S.V. Peletminskii. *Spin Waves* (John Wiley & Sons, North-Holland, Amsterdam, 1968)
[25] M.A. Lavrent'yev, B.V. Shabat. *Metody teorii funktsiy kompleksnogo peremennogo* (Nauka, M., 1987) (in Russian).
[26] G.N. Watson. *Theory of Bessel Functions* (Cambridge University Press, 1922)
[27] A.K. Andreev. Tech. Phys. Lett., **47** (6), 547 (2021). DOI: 10.1134/1955S1063785021060031
[28] G. Eason, B. Noble, I.N. Sneddon. Phil. Trans. Roy. Soc., Lond. A, **247** (935), 529 (1955).
[29] Y.L. Luke. *Mathematical Functions and Their Approximations* (Academ. Press Inc. NY., San Francisco, London, 1975)
[30] A.K. Andreev. Tech. Phys. Lett., **46** (11), 1096 (2020). DOI: 10.1134/S1063785020110024
[31] A.K. Andreev. Tech. Phys. Lett., **47** (5), 464 (2021). DOI: 10.1134/S1063785021050023
[32] S.G. Kalashnikov. *Elektrichestvo* (Fizmatlit, M., pp 2003) (in Russian).
[33] A.H. Bobeck, E. Della Torre. *Magnetic Bubbles* (North-Holland Publishing Company-Amsterdam, Oxford, 1975)
[34] H. Callen, R.M. Josephs. J. Appl. Phys., **42** (5), (1977). DOI: 10.1063/1.1660475
[35] A.K. Andreev. J. Machinery Manufacture and Reliability, **51** (6), 511 (2022). DOI: 10.3103/S1052618822060036
[36] I.V. Savel'yev. *Kurs obshchey fiziki*, kn. 2. *Elektrichestvo i magnetizm* (Lan', SPb., 2006) (in Russian).
[37] M. Abramowitz, I. Stegun (ed.). *Handbook of Mathematical Functions* (Nation. Bureau of Standards, NY., 1964)

Translated by 123